第32卷 第8期 焊 接 学 报 Vol. 32 No. 8
2011年8月 TRANSACTIONS OF THE CHINA WELDING INSTITUTION August 2011

基于 MATLAB 的球管相贯空间曲线焊缝的数学模型

赵 洁[1,2]， 胡绳荪[1,2]， 申俊琦[1,2]， 陈昌亮[2]， 丁 炜[1]

(1. 天津大学 天津市现代连接技术重点实验室，天津 300072;
2. 天津大学 材料科学与工程学院，天津 300072)

赵 洁

摘 要：核电压力容器的焊接中，球面与圆管相贯复杂空间曲线焊缝的自动化焊接是焊接领域的难题，构建该相贯线焊缝的数学模型是研究其焊接问题的前提条件. 研究结合球管相贯焊缝的实际情况采用 MATLAB 软件建立了球管相贯线焊缝的数学模型，将实际空间相贯线简化为平面曲线；考虑壁厚影响，通过增加球径和管径两个方向上的修正量 $\triangle D$ 和 $\triangle d$，对 J 形坡口焊缝模型作出修正. 结果表明，通过 MATLAB 软件编程产生的可独立运行的图形用户界面 GUI 能够完成模型绘图、数据输出等功能，从而为该形状焊缝的机器人焊接与控制提供理论依据.

关键词：自动化焊接；球管相贯线；数学模型；图形用户界面

中图分类号：TG409 **文献标识码**：A **文章编号**：0253－360X(2011)08－0089－04

0 序 言

实现高质量、高效率的焊接是核电制造工程中的基本要求. 为了加快核电设备的建设，必须在核电设备制造中推广先进的焊接工艺与焊接自动化技术. 在大型压力容器和管道工程应用中，复杂相贯线焊缝是十分常用的典型焊缝形式. 这种空间曲线焊缝焊接劳动强度大、焊接质量不易保证，因此越来越多地采用机器人进行焊接.

目前，国内外对空间曲线机器人焊接的研究与应用主要集中在管－管相贯所谓“马鞍形”焊缝[1,2]自动焊接方面，而且一般是进行圆管外壁相贯焊缝的焊接. 球内壁与管相贯“马蹄窝”焊缝比管与管相贯“马鞍型”焊缝形状更加复杂，而且由于受到空间位置的限制，该焊缝机器人焊接的困难可想而知. 该结构焊缝目前都采用焊接质量与效率较低的手工焊方法进行焊接. 文中旨在建立圆管与球面相贯空间曲线的数学模型，运用软件编程绘图，得到具有一般性的相贯线焊缝轨迹及相关数据，为核电压力容器及其它工程结构中球面与圆管相贯焊缝机器人焊接与控制提供理论依据. 球管相贯焊接自动化的实现对于满足焊接工程高质量、高效率的需求，促进国家核电压力容器设备制造自主化、国产化具有重要意义.

收稿日期：2010－11－28
基金项目：国家自然科学基金资助项目(50975195)；天津市自然科学基金资助项目(10JYBJC06500)

1 球管相贯线的数学模型

1.1 数学模型准备

由于核电压力容器封头与多个圆管相贯，不同的圆柱管直径、球面曲率和球面位置，会得到不同的相贯线形状. 为解决工程实际问题，就必须建立能够反应不同曲率球面、不同直径圆管在球面不同位置的相贯线数学模型，即要求研究要具有一般性.

骑座式机器人焊接[3]中，往往是围绕圆管的中心线进行相贯线的焊接，因此，所建立的球面与圆管相贯焊缝轨迹的数学模型，必须转换为以圆管中心为参考轴的空间焊缝轨迹数学模型，该模型才是机器人焊接中的焊枪运动轨迹模型. 实际焊缝 J 形坡口的空间立体，假设先不考虑 J 形坡口尺寸和形状的影响，实际焊缝的数学模型简化为球内表面和管外表面相贯形成的一条空间相贯线.

1.2 球管相贯线方程的推导

如图 1 所示建立坐标系，yOz 与 $y'O'z'$ 位于同一平面，以球心 O 为原点，建立直角坐标系 O-xyz 以圆柱面轴线与球面的交点 O' 为原点，建立直角坐标系 O'-$x'y'z'$.

经过坐标变换等运算，推导得相贯线在 O'-$x'y'z'$ 坐标系中的参数方程为

$$\left.\begin{aligned} x' &= r\cos\alpha \\ y' &= r\sin\alpha \\ z' &= -\sqrt{R^2-\left[(r\cos\alpha)^2+(r\sin\alpha+e)^2\right]}+\sqrt{R^2-e^2} \end{aligned}\right\} \quad (1)$$

式中: R 为球面半径; r 为圆管半径; e 为两者轴线间的距离; α 为某点和原点 O' 连线在 $x'O'y'$ 平面内的投影,与 x' 轴的正半轴的夹角变化范围为 $0 \sim 2\pi$.

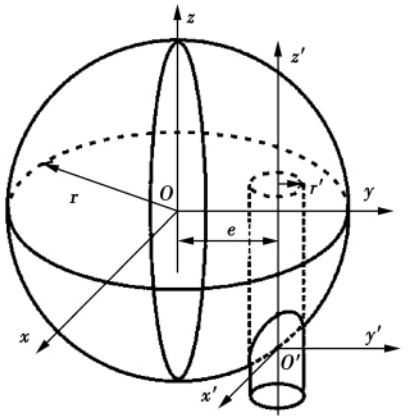

图 1 坐标系示意图

Fig. 1 Schematic diagram of coordinate system

式(1)即为所建立的相贯线在 O'-$x'y'z'$ 坐标系中的参数方程.

可得,解析方程为

$$z' = -\sqrt{R^2 - [x'^2 + (y'+e)^2]} + \sqrt{R^2 - e^2} \quad (2)$$

2 结合 MATLAB 软件的数学建模

2.1 基本功能的实现

MATLAB 提供了三维绘图函数,可以直观地从各个角度观察绘制出的三维图形,是一套高性能数值计算和可视化软件[4]. 在 MATLAB 中,运用将曲面分为面片的思想绘制出了球管相贯曲线的数学模型,见图 2.

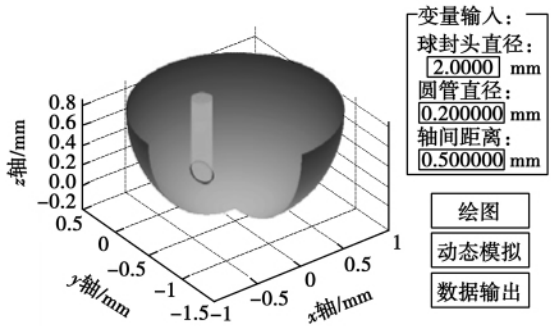

图 2 球管相贯示意图

Fig. 2 Schematic diagram of intersection of sphere and tube

球面对应的部分程序代码如下:

```
theta = (88/180:.0001:92/180) * pi + acos(e/R);
phi = (-2* atan(r/e):.001:2* atan(r/e)) + pi/2;
x = zeros(length(theta),length(phi));
y = x;
z = x;
for i = 1:length(theta)
   for j = 1:length(phi)
      x(i,j) = R* sin(theta(i)) * cos(phi(j));
      y(i,j) = R* sin(theta(i)) * sin(phi(j));
      end
      z(i,:) = R* cos(theta(i));
end
surf(x,y-e,z+sqrt(R^2-e^2));
……
```

并且根据 MATLAB 工作空间中相贯线上点对应的变量值验证得,所求理论相贯线方程是正确的.

2.2 创建图形用户界面

在 MATLAB 命令窗口中即可以实现绘图及提供模型所需数据. 但是需要用户熟悉 M 文件编程、参数传递及数据导出等. 为方便用户使用,文中在 MATLAB 中创建了一个友好的界面 GUI(graphics user interface),它的执行效率更高,用户不需要知道应用程序是怎样执行各项命令的,只需了解可见界面组件的使用方法,即可得到所需结果. 文中选用图形 FIG(figure) 方式创建 GUI 界面[5]. 设计得到的界面,能够实现当输入三个已知变量值球面直径 D,圆管直径 d,两者轴线间的距离 e 时,即可输出所需要的相贯线方程和线上点的坐标值; 当用户输入微调量,即可得到多层多道焊缝模型所需的数值.

由于 MATLAB 软件庞大、占用空间大,故借助 MATLAB Deployment Project 将 GUI 转化为独立于 MATLAB 平台的应用程序. 即在没有安装该软件的环境下也能运行,比较便捷. 实际尺寸相贯焊缝的图形用户界面,如图 3.

3 数学模型检验与应用分析

考虑到 J 形坡口加工中所用铣刀刀具为平面形状及实际管径比球径小很多等情况,对空间相贯线进行了平面度分析[6]. 首先确定相贯线的理想接近平面,求解得相贯线上的点距该平面的最大距离,最后对绘图结果分析得在焊接领域该最大距离误差(1.561 1 mm)可以忽略,即可将该相贯线视为平面曲线. 并对模型可以简化为平面曲线的条件进行了

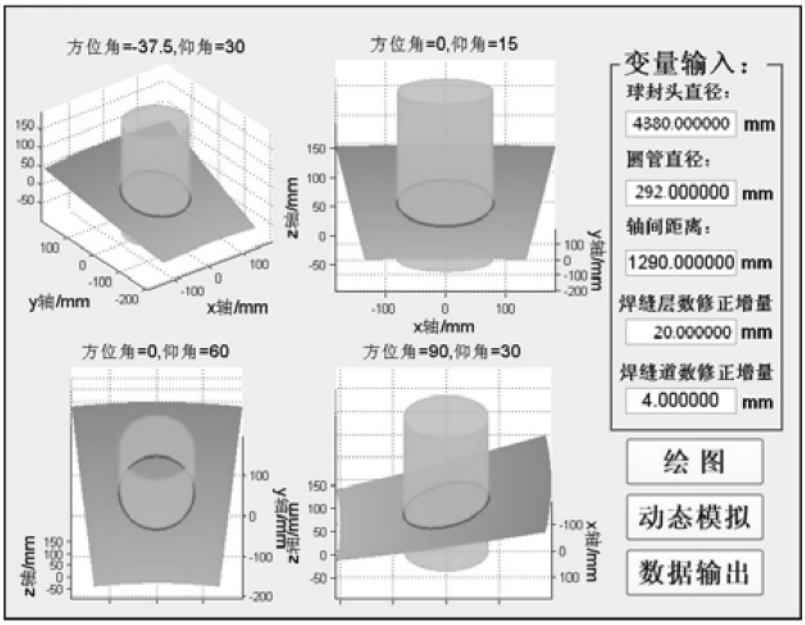

图 3　实际尺寸相贯焊缝图形用户界面

Fig. 3　GUI of Intersection seam of actual size

进一步的分析. 由中值法原理依次计算,得 R: $r \geqslant 15$ 均可满足要求.

在某一特定管的焊接过程中,简化模型的数学计算过程更快,执行控制效率更高,在平面内进行焊接的控制比在空间简单. 故相贯线可以视为平面曲线这一结论,对于该课题机器人焊接的控制具有重要意义.

实际焊接过程中,由于封头壁厚的影响,仍需考虑 J 形坡口形状与大小等因素. 由于相贯线模型是一个 J 形坡口多层多道的"马蹄窝"型空间立体,需要对不同道的焊缝模型进行参数微调,J 形坡口焊缝的模型可以作出如下修正:

图 4 为某管相贯焊缝剖视图,球内表面直径 D,圆管外表面直径 d,两者轴线间的距离 e. 设对于 J 形坡口焊缝剖面下半部分的某层某道焊缝,考虑壁厚的影响,模型需在球径方向经过修正方可使用,设 $\triangle D$ 为前一层焊缝表面距离球内表面的距离,分析知,将模型中的 D 变为 $D' = D + 2\triangle D$,即可得到该焊缝的模型. 亦可设 J 形坡口总深度为 δ,每层焊道厚度约为 $\triangle\delta$,则第 x 层的 $D' = D + 2(\delta - (x-1) * \triangle\delta)$,用 D' 代换 D 得到模型.

可以看出,J 形坡口焊缝仍需在管径方向做进一步修正,同理,将模型中的管径 d 变为 $d + 2\triangle d$,得到修改后模型.

经过球径和管径两个方向上的修正即可得到实际 J 形坡口多层多道焊缝的模型. 其中变量 $\triangle D$,

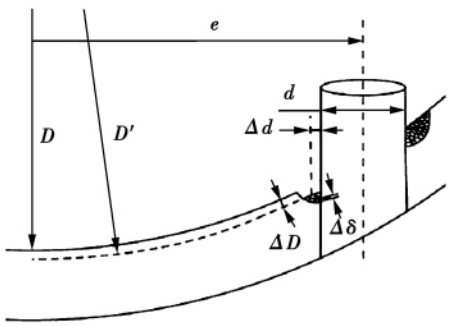

图 4　管相贯焊缝剖视图

Fig. 4　Cutaway view of intersection seam of a certain tube

$\triangle d$ 可视为焊缝层数和焊缝道数的修正增量,可以由界面输入.

4　结　　论

(1) 该球管相贯曲线模型的建立,具有一般性. 并得出实际尺寸相贯线焊缝可以视为平面曲线.

(2) 对 J 形坡口焊缝模型在球径和管径方向上作出修正,能够满足实际多层多道焊焊缝的需要.

参考文献:

[1] Masatoshi Hida, Akira Okamoto, Toshihiko Nishimura, *et al*. Development of automatic welding system for crawler crane latticed booms [J]. Kobelco Technology, 2007, 27: 53 - 57.

[2] 胡中华，陈焕明，熊震宇，等. 弧焊机器人马鞍形工件焊枪姿态规划研究[J]. 机械与电子，2007(4)，10－13.
Hu Zhonghua，Chen Huanming，Xiong Zhenyu，*et al*. Study on torch pose planning of arc welding robot for saddleshape workpiece [J]. Machinery and Electronics，2007(4)：10－13.

[3] 李晓辉，汪 苏. 骑座相贯线焊接机器人运动学分析及仿真[J]. 北京航空航天大学学报，2008，34(8)：964－968.
Li Xiaohui，Wang Su. Kinematic analysis and simulation of saddle-back coping welding robot [J]. Journal of Beijing University of Aeronautics and Astronautics，2008，34(8)：964－968.

[4] 唐昌建. MATLAB 编程基础及应用[M]. 四川：四川大学出版社，2003.

[5] 施晓红，周 佳. 精通 GUI 图形界面编程[M]. 北京：北京大学出版社，2003.

[6] 史立新，朱思洪. 基于 MATLAB 的平面度误差最小区域法评定[J]. 组合机床与自动化加工技术，2005(9)：58－59.
Shi Lixin，Zhu Sihong. The minimum zone method of flatness error based on Matlab [J]. Modular Mashine Tool & Automatic Manufacturing Technique，2005(9)：58－59.

作者简介： 赵 洁，女，1988 年出生，硕士. 主要从事焊接领域自动化技术的研究. 发表论文 2 篇. Email：zhaojie@tju.edu.cn

通讯作者： 申俊琦，男，讲师. Email：shenjunqi@tju.edu.cn

welding process and welding stirring pin shape are the key of high-quality fillet welding joint. When the rotation speed is 30 – 40 rad/s and the welding speed is 90 – 120 mm/min, we can get a high-quality weld appearances.

Key words: friction stir welding; outer fillet welding; 2519 aluminum alloys

Ultra-high cycle fatigue behaviors of Q345 bridge steel welded joint FANG Donghui[1], LIU Yongjie[2], CHEN Yiyan[3], WANG Qingyuan[2] (1. Department of Civil Engineering & Architecture, College of Jincheng, Sichuan University, Chengdu 610065, China; 2. Department of Mechanics and Engineering Science, Sichuan University, Chengdu 610065, China; 3. Shenzhen Municipal Design & Research Institute, Shenzhen 518029, China). p 77 – 80

Abstract: The high cycle and ultra-high cycle fatigue properties of Q345qC base metal and circular butt weld joint were studied by using the ultrasonic fatigue testing technique. The experimental results show that during $10^5 - 10^9$ cycles, the fatigue strength of welded joint is much less than that of base metal, and both their S-N curves descend continuously. Fracture can still occur on base metal beyond 10^7 cycles and on welded steel beyond 5×10^6 cycles. The observation of fracture surface shows cracks mainly initiate from welded toes at fusion area or geometric discontinuity at the surface in welded steel. Furthermore, fatigue failure occurs at the geometric discontinuity area in the high stress regime but occurs at welded toes in the low stress regime.

Key words: ultra-high cycle fatigue; welded joint; ultrasonic fatigue test; S-N curve; fracture surface

Numerical simulation of dynamic laser melting behavior and temperature field on cast iron surface YI Peng, LIU Yancong, SHI Yongjun, JIANG Hao (College of Mechanical and Electronic Engineering, China University of Petroleum, Dongying 257061, China). p 81 – 84

Abstract: For explicitly understanding the thermo-mechanism of laser melting process on cast iron, a validated dynamic three-dimensional numerical modal for this process was established by taking into account the thermal physical parameters and latent heat of the material. The temperature field and the relationships between different process parameters were studied with this model, and the simulation results were in accordance with the experimental results. The results indicate that the penetration depth of the laser melting process on cast iron is grater than that on the steel. The large temperature gradients inside and outside the molten pool are dominated by the depth and width components respectively. A larger temperature gradient is gained through reducing scan speed and spot size. The pool is shrunk by the increase of scan speed and spot radius; the solidification speed is raised with the increase of laser scan speed and reduction of the spot size.

Key words: laser melting process; cast iron; numerical simulation; transient temperature field; molten pool

Microstructure and properties of Er-containing aluminum alloy TIG weld joints JIN Likun[1], LI Xiaoyan[1], HE Dingyong[1], JIANG Jianmin[1], YANG Dongxia[2], NIE Zuoren[2] (1. College of Materials Science and Engineering, Beijing University of Technology, China; 2. New Functional Materials Key Laboratory of Ministry of Education, Beijing University of Technology, Beijing 100124, China). p 85 – 88

Abstract: To study the strengthening effect and mechanism of Er element on the weld, the remelting welding of Al-Mg alloy with Er was adopted, and the organizational structure and mechanical properties of the joint were observed. The results show that there is primary Al_3Er phase precipitation on the grain boundaries in weld, but the quantity of it is fewer than that of in the base material, and the precipitation doesn't form a continuous ring. The secondary Al_3Er precipitation also can be found in the welding, but the precipitation phase quantity is very few. Er elements will presence in the solid solution or segregation way. The strength of Er element on the weld joint is mainly based on the primary Al_3Er to refine the grain. The effect of the secondary phase on the weld joint is small, and so the weld joint mechanical properties decrease evidence. The tensile strength of welded joints is 297 MPa, and the strength coefficient of welded joints is 72% of base material. Tensile fracture position is mainly in the center of the weld and near the fusion zone.

Key words: primary phase; secondary phase; fine-grain strengthening; precipitation strengthening

Mathematical model based on MATLAB for intersection seam of sphere and tube ZHAO Jie[1,2], HU Shengsun[1,2], SHEN Junqi[1,2], CHEN Changliang[2], DING Wei[1] (1. Tianjin Key Laboratory of Advanced Joining Technology, Tianjin University, Tianjin 300072, China; 2. School of Materials Science and Engineering, Tianjin University, Tianjin 300072, China). p 89 – 92

Abstract: The welding process of complex space curve, such as intersection seam of sphere and tube, is difficult in the field of welding automation, and the construction of a mathematical model of intersection seam is a prerequisite for the welding process. After a mathematical model of intersection curve of sphere and tube is established with MATLAB software, by further analysis, the intersection curve can be simplified to plane curve. By considering the thickness effects of the sphere, some amendments to the model of J-shaped groove weld are made by increasing $\triangle D$ and $\triangle d$ two corrections in the diameter directions of sphere and tube respectively. All functions such as graphics and output data, are integrated into a GUI (Graphics User Interface) based on MATLAB programming, and the GUI is converted to a standalone application which is efficient and convenient, which provided a theoretical basis for robot welding and controlling of this seam weld.

Key words: welding automation; intersection curve of sphere and tube; mathematical model; graphics user interface

Influence of different cooling rates on microstructure of Ti-6Al-4V titanium alloy thermal simulation specimens WANG Jinlin[1], GAN Zhanghua[1], CHEN Yiming[1], XIAO Jianzhong[2] (1. College of Materials Science and Metallurgical Engineering, Wuhan University of Science and Technology, Wu-